

# Error grid analysis evaluation of noninvasive blood glucose monitoring system of diabetic Covid-19 patients

Lina Nasseer Bachache<sup>a,\*</sup>, Auns Qusai Al-Neami<sup>a</sup>, Jamal A. Hasan<sup>a</sup>

<sup>a</sup>Biomedical Engineering Department, College of Engineering, Al-Nahrain University, Baghdad, Iraq

(Communicated by Madjid Eshaghi Gordji)

---

## Abstract

Due to the life-threatening dangers of diabetic disease and the rapid spread of the Corona pandemic, the demand for continuous glucose monitoring systems increases, especially that complemented with telemedicine technologies. During and after the corona pandemic, the number of diabetes patients is anticipated to rise rapidly. This study aims to learn the interaction between diabetes and COVID-19 and the health complication, owing to control blood glucose levels to decrease these complications. Careful blood sugar control is essential because the poorer health results are strongly linked with greater blood sugar levels in COVID-19 infection patients. The non-invasive glucose detection system is vital to control diabetic COVID-19 patients' health cases. The non-invasive blood glucose monitoring system is based on acousto-optic Raman-Nath interaction using 2MHz ultrasound and 980nm IR laser. Clark's Error Chart and Parkes Error Grid are used for evaluating the non-invasive blood glucose monitoring system and show a promising evaluation result.

*Keywords:* Clark's Error Chart, Parkes Error Grid, Diabetic, COVID-19, Blood glucose detection, Noninvasive detection, Acousto-optic, NIR, Thin piezoelectric crystal.

---

## 1. Introduction

The severity of COVID-19 increase with diabetic patient and their blood glucose elevation. COVID-19 is an acronym for corona virus disease that appeared in 2019. Coronavirus is enclosed, positive single-stranded giant RNA viruses infect humans and animals. Tyrell and Bynoe studied and

---

\*Corresponding author

Email addresses: [lina\\_nasseer@yahoo.com](mailto:lina_nasseer@yahoo.com) (Lina Nasseer Bachache), [uns\\_alneami@eng.nahrainuniv.edu.iq](mailto:uns_alneami@eng.nahrainuniv.edu.iq) (Auns Qusai Al-Neami), [jamalabduljabar@eng.nahrainuniv.edu.iq](mailto:jamalabduljabar@eng.nahrainuniv.edu.iq) (Jamal A. Hasan)

Received: November 2021 Accepted: January 2022

grew the viruses extracted from patients with common colds, initially characterized coronaviruses in 1966. They were named coronaviruses from the Latin word corona, which means crown. Their shape is spherical virions with a core-shell and surface projections resembling a solar corona. Coronaviruses are divided into four subgroups: alpha, beta, gamma, and delta. While alpha and beta coronaviruses are thought to have originated in mammals, particularly bats, gamma and delta viruses are thought to have originated in pigs and birds. Beta coronaviruses, one of the coronavirus subtypes that may infect humans, can cause severe sickness and death, whereas alpha coronaviruses induce asymptomatic or slightly symptomatic infections [12, 4].

COVID-19 is a member of the beta coronavirus family. COVID-19 is also called SARSCoV2 (severe acute respiratory syndrome coronavirus number two). The current COVID-19 outbreak, which began in Hubei Province of the People's Republic of China, has spread to other nations. On the Huanan seafood market in Wuhan, China, SARSCoV2 appears to have transferred from animals to people. Based on rising case notification rates in Chinese and worldwide locales, the WHO Emergency Committee declared a global health emergency on January 30, 2020 [12].

Diabetes is a chronic disease with the hallmark of hyperglycemia in both fasting and after eating. This failure in regulating blood sugar is due to a deficiency in insulin hormone [17]. Several organ damages, malfunction, and loss in organs and tissues such as the retina, kidney, neurons, heart, and blood vessels are all linked to the chronic hyperglycemia of diabetes disease [21]. In the initial type two diabetes, molecular mechanisms attenuate the effect of insulin and produce the state of insulin-resistant [19]. Insulin resistance is the low biological response to a typical or elevated insulin level. Insulin resistance makes compensatory hyperinsulinemia, which increases the secretion of beta cells, to keep the normal BGL, which has been produced overwork of pancreas and diabetes in the future [24].

Due to the rising number of COVID-19 patients and many diabetic patients with corona infection, it is critical to understand the unique characteristics of COVID-19 disorder in persons with diabetes and the complication relationship with glucose level fluctuations [18]. Noninvasive blood glucose testing becomes more crucial to monitor glucose levels many times a day or more to arrive at the optimum pharmacological approach for diabetes glucose control [22]. COVID-19 has an increasing number of disturbing psychological consequences over the world. COVID-19 patient has Coronaphobia, which causes despair and anxiety and prevents medical health care providers from monitoring glucose levels invasively numerous times a day since the unpleasant intrusive procedure might exacerbate the situation. Glucose monitoring and control are critical for preventing the condition from deterioration [9]. Corona pandemic accelerates the need for telemedicine technologies to monitor the glucose level of diabetic patients, which could be linked to the existence of noninvasively blood glucose level monitoring [18].

## 2. Error Grid Analysis

Analytical accuracy and clinical accuracy are two ways to define the performance of the blood glucose (BG) meter. The discrepancy between blood glucose levels obtained with a reference technique and blood glucose values obtained with a blood glucose meter assessed is analytical accuracy. Linear regression is a standard method for improving analytical accuracy, and common metrics include the percentage deviations and coefficient of correlation. These metrics are inappropriate for describing clinical accuracy since they cannot detect significant outliers, and the clinical outcome of treatment decisions depends on blood glucose meters with percentage variations highly dependent on the blood glucose level. Clinical accuracy is a qualitative way of describing blood glucose meter accuracy, whereas analytical accuracy is quantitative. The discrepancies between the blood glucose

meter results and the actual reference blood glucose value were used to assess the outcomes of treatment decisions. The error grid analysis is a commonly used method for clinical accuracy. Pairs of data from the blood glucose meter and the reference technique were displayed on the error grid for the analysis. A set of risk zones is usually overlaid on that graph. Each zone reflects the likelihood of a negative consequence due to the measurement inaccuracy in blood glucose levels. Analyzing an error grid determines the percentage of data points that fall into each clinical outcome zone [8].

### 2.1. Clarke Error Grid

Clarke error grid analysis is a standardization method that measures the clinical accuracy of a patient's new blood glucose meter device versus the blood glucose value acquired from the reference standard meter used. In 1987, Diabetes Care published the Clarke error grid analysis description. This comparison evaluated the clinical accuracy of meter-generated blood glucose estimations to a reference value. The error grid analysis ultimately became one of the "gold standards" for assessing the accuracy of blood glucose meters. The Clarke Error Grid was developed by five (university of Virginia) specialists based on clinical experience. The specialists all came to the same conclusion: The patient's BGL was established to be between 70 and 180 mg/dl as a target range. Patients are well managed within this range; patients must intervene with remedial activities below this range. A correction results in a BGL outside the intended domain will fail to handle a BGL outside the target range were both deemed improper. The experts' decisions result in a five-zone error grid called zone A through E. Figure 1 shows the Clarke Error Grid. The area on both sides of the diagonal is known

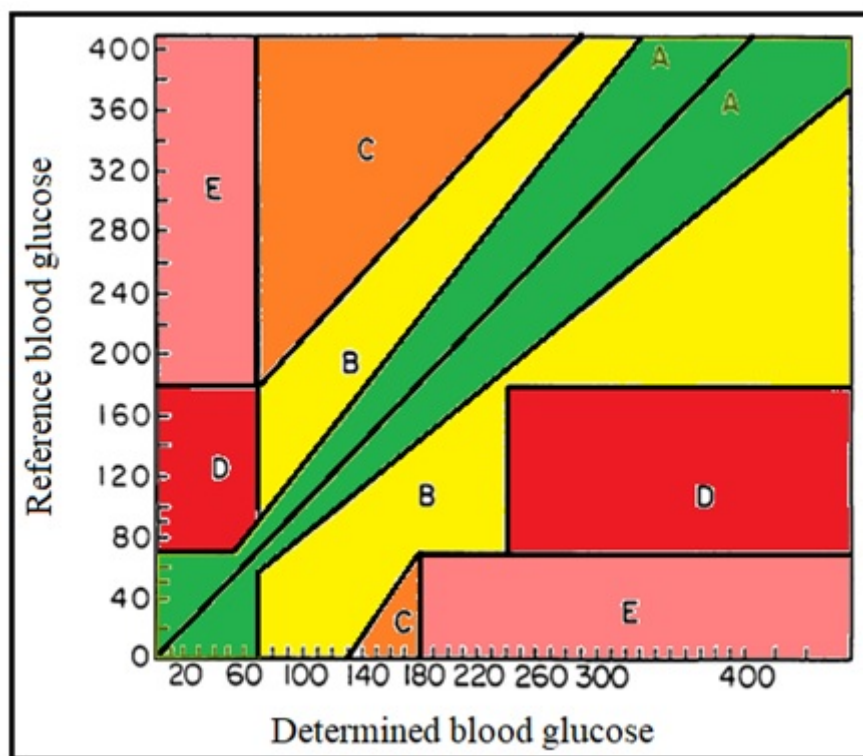


Figure 1: shows the Clarke Error Grid [20],edited .

as Zone A. The design of the zone is based on the assumption that a discrepancy of less than 20% between blood glucose meter and reference BGL readings, or BGL values and reference values in the hypoglycaemic range less than (70mg/dl), leads to clinically accurate judgments by users. On

the other hand, it is very hazardous if the values obtained with the blood glucose meter cause the incorrect choice about how to handle the actual BGL measured by the reference technique. Based on the meter readings, the correction is an insulin bolus if the blood glucose meter detects BGL over 180mg/dl while the reference value is below 70mg/dl. This management would be a poor choice, and the patient would be pushed deeper into hypoglycemia (upper left zone E). If the actual BG is over 180mg/dl and the BG blood glucose meter readings are below 70mg/dl, the therapeutic choice increases the blood glucose instead of increasing insulin (lower right zone E). Zone D is defined as the zone when blood glucose meter readings are in the goal range of (70-180) mg/dl, but reference values are less than 70 mg/dl or more than 180 mg/dl. A correction is not required based on the blood glucose meter readings, but one is needed based on the actual values of the reference method, particularly in the hypoglycaemic range. The required adjustments are not triggered by the blood glucose meter readings in Zone D. Zone C, on the other hand, has a real value that is more than 100mg/dl lower than the BGL of meter for blood glucose meter readings over 180mg/dl (upper C). The reasonably tiny zone C (lower C) includes all BGL readings in the hypoglycaemic range, matching reference values between 130 and 180mg/dl. The BGL in both zones leads to over-corrections, with a correction with an excessively high dosage of insulin in upper C and an adjustment with a massive adjustment to increase blood glucose in lower C. The discrepancy between blood glucose meter and reference readings is more than 20% in the remaining zone B. As a consequence, the clinical choices made are not accurate (zone A) but uncritical. As a result, the Clark-Error Grid divides into five zones: A: Clinically proper judgments, B: Clinically uncritical judgments, C: Overtreatment, D: Skipping a required correction, E: Applying the opposite and wrong decisions [20].

## 2.2. Parkes Error Grid

It was criticised considering the Clark Error Grid's tremendous use and widespread acceptance. For example, the Clark Error Grid was only presented by a limited number of specialists. There are abrupt transitions between zones, such as the direct transition between zone B and zone E skipping zones C and D. In addition, the Clark Error Grid does not distinguish between types 1 and 2 diabetes. All of this leads to a new description of the Error Grid's five zones 13 years later: In 1994, during the American Diabetes Association (ADA) annual conference, 100 doctors were asked to evaluate the boundaries of the five risk zones (0–4) for type 1 and type 2 diabetes patients individually as shown in figure 2. The mean values of the danger zones are from 0 to 550mg/dl in increments of 10mg/dl with smoothed boundaries using the two times 100 individual Error Grids. The Parkes Error Grids or Consensus Error Grids for type 1 diabetic patients (A) and type 2 diabetic patients (B) are the results (B). The two types of grids have just minor changes. Zone A is a little narrower for people with type 1 diabetes, and zone B is slightly broader. Zone B/C and zone C/D have a lot of similarities in terms of their boundaries. The Parkes Error Grid, in contrast to the Clark Error Grid, features smooth transitions between zones, a more comprehensive range up to 550mg/dl, and no lower zone E [13].

## 3. Interaction of Diabetic with COVID-19 and their Complications

Careful blood sugar control is essential in COVID-19 infection patients because the poorer health results of the infected patient are strongly linked with greater blood sugar levels, and It was possible to anticipate the severity of the infection if the glucose level is severely elevated [16]. This increase in severity is linked to the inhibition of innate and humoral immune mechanisms [23]. Also, other pulmonary bacterial infections are complicated and become more dangerous in diabetic patients [11]. The risk of patients needing to stay in the intensive care unit is duplicated several times if they have

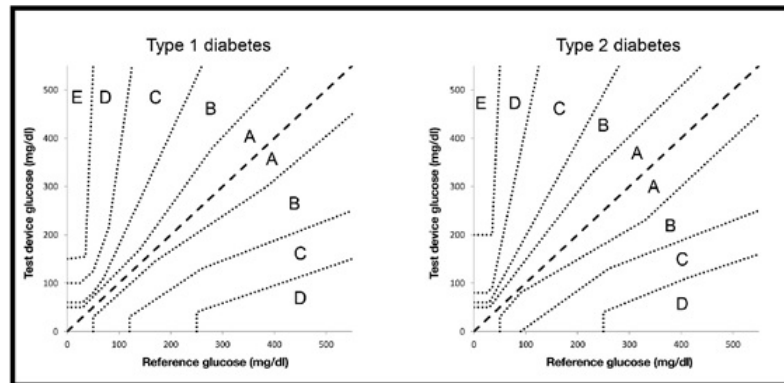


Figure 2: Parkes Error Grid [13].

diabetes. Diabetes causes poor neutrophil chemotaxis and phagocytosis, which facilitates the spread of germs and lengthens the time it takes for germs to be cleared [23]. Diabetes is also linked to increasing furin that simplified COVID-19 virus proliferation [1]. Increased angiotensin-converting enzyme II may make individuals with diabetes more susceptible to SARS CoV2 infection. In non-diabetic patients infected by severe acute respiratory syndrome (SARS), the first coronavirus induces hyperglycemia due to the viral receptors expressed in pancreatic islets [2]. Severe diabetes produce lymphocytopenia, which depresses the immune system response to COVID-19 [7]. Corona pandemic accelerates the need for telemedicine technologies to monitor the glucose level of diabetic patients, especially with depression, due to staying home, which produces a dietary change and increases the intake of high-calorie food. During and after the corona pandemic, the number of diabetes patients is anticipated to rise rapidly [16, 23].

The elasto-optic effect, the optical properties changing as a reaction to the applied ultrasound, provides the foundation for acousto-optic interaction. A piezoelectric transducer transmits the acoustic signal into the tissue, and the acoustic, elastic wave causes compression and rarefaction zones. A frequency shift occurs when an optical, electromagnetic beam passes through a tissue sample and is modified or deflected. Due to medium straining, the refraction index of the medium changes. The interaction sample material's wavelength of light and sound, interaction geometry, and optical and acoustic characteristics determine the kind of acousto-optic interaction. Human tissue is an anisotropic medium that alters the polarization of optical beams, resulting in multiple (Raman-Nath regime) or single diffracted optical beams (Bragg regime). The Bragg regime is significantly more efficient but more challenging to execute; the acousto-optic system is very useful in glucose monitoring noninvasively [3].

#### 4. Experiments

Noninvasive glucose detection using an acousto-optic system with Raman-Nath regime by applying infrared laser with 980nm of 10 mill-watt power to the patient finger orthogonal to ultrasound crystal of 2 megahertz (that generated from and thin piezoelectric crystal (LDT0-028) after being connected to an alternative voltage function generator) and measure the penetrated infrared through the finger as shown in figure 3. When the laser beam interacts with human tissues, it is diminished by scattering in addition to tissue absorption, but ultrasound waves decrease light scattering and increase light penetration. And GY-906 is selected as a sensitive near-infrared detector. The measured data are calibrated to neglect the user body temperature and other abundant IR energy, represented in Equation1. Where mainly selected  $N = 10$  to bypass the fault measurement, initial sensor reading

is the sensor reading before operating the IR source and ultrasound. This reading is the collected IR from the user body temperature and abundant temperature and light. While the microcontroller is used to operate the sensor and process the light data and prepare glucose measurements to display the system.

#### 4.1. GY-906

It is a non-contact infrared-sensitive temperature sensor, capable of sensing between 70°C–380°C with a resolution of 0.02°C. , this sensor will measure the penetrated IR light through the patient finger [15]. Firstly measure the collected infrared data of patient body temperature and the ambient temperature and light without operating the infrared source and then neglected the common signal to eliminate the unwanted interference signal from the correlated glucose signal according to equation (4.1)

$$\text{Glucose measurement} = \frac{1}{N} \sum_{i=1}^N \text{Sensor reading } (i) - \text{Initial sensor reading} \quad (4.1)$$

Where primarily selected  $N = 10$  to neglect the fault measurement, initial sensor reading is the sensor reading before operating the IR source; this reading is the collected IR from the user body temperature and abundant temperature and light.

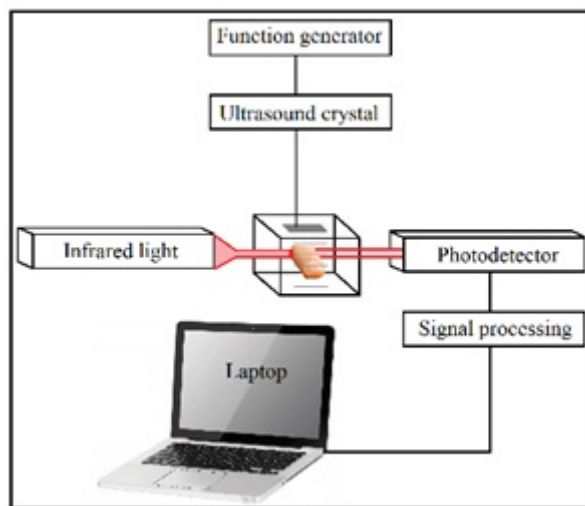


Figure 3: Acousto-optic Glucose detection system.

#### 4.2. IR 980nm

Infrared laser diode that emits light with a dominated wavelength of 970-990 nm that is suitable for detection glucose level with operating voltage of (1.5 to 2.2) volt, and operating current of (25 to 40) mA, the radius of the emitting beam is 3.6mm [5]. The maximum irradiance of light is 98.2 mW/cm<sup>2</sup> if the maximum power is ten milliwatts and the diameter of the diode is 3.6 mm. This maximum power is lower than the maximum acceptance power (150 mW/cm<sup>2</sup>), and the maximum thermal acceptable fluence of laser light-limited to 200 J/cm<sup>2</sup> means the maximum applied time is limited to 33 minutes to avert unwanted thermal effects [14].

### 4.3. LDT0-028

The implemented LDT0-028 piezo film sensor is shown in figure 4. It is a grove piezo film sensor made from a polymer material that is flexible, lightweight, tough, and has a low acoustic impedance that is closer to the acoustic impedance of water and human tissue. This thin film of PVDF is a transducer that can convert electrical energy into ultrasound mechanical energy [6]. We used an ultrasound generator to produce two megahertz ultrasound radio waves. We choose two megahertz ultrasound radio waves due to their excellent penetration in human tissue [10].



Figure 4: LDT0-028 piezo film [6]

## 5. Result and discussion of detection blood glucose level of normal people and diabetic patients that are infected by COVID-19 disease

The glucose measuring systems of the experiment are tested by measuring the blood glucose magnitude of four COVID-19 patient volunteers and 280 samples. For two weeks, taking each patient's measurements five times (the time between the measurements is approximately one hour), all the non-invasive measurements are compared to invasive measurements, as shown in Figure 5. The root means square errors are calculated by measuring the root square of the difference between the prototype measurements and the invasive reference measurement for each BGL measurement and produce RMS (Root Mean Square Error) equal to (98.0119) mg/dl and maximum error equal to (226) mg/dl as demonstrated in Figure 6. Finally, this glucose detection prototype system is evaluated for COVID-19 patients using the Clark error chart as shown in Figure 7 and the Parkes error grid as shown in Figure 8. Clark's error chart shows three measurements in the D region, 31 in the B region, 217 in the A region, and 29 out of regions. That means 1.1 % of measurements produce potentially life-threatening decisions that fail to recognize hyperglycemia, 11.07 % are wronged, but lead uncritical judgments, 77.5 % of measurements make the right decisions, and 10.36 % are out of the Clarke evaluation system. Parkes error grids show 50 measurements in the B region, 223 in the A region, and 7 out of regions. Parkes error grids show that 17.86% are drifted and lead to uncritical judgments 79.64 % of measurements make the right decisions, and 2.5% out of Parkes evaluation system can produce drifted measurements and lead to the unprecise drug of choice. That means the prototype system has good evaluation results for COVID-19 patients but with a shift in the high-level measurements that may be caused by the COVID-19 effects and symptoms but also this glucose measuring prototype system (AO measuring system based on 980nm and 2MHz ultrasound) still in acceptable Parkes evaluation system.

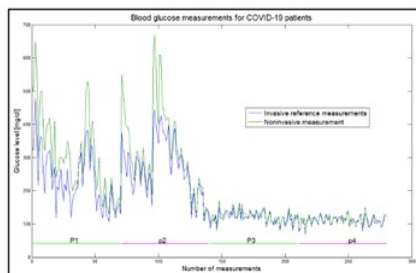


Figure 5: Comparison between noninvasive BGL measurements based on AO interaction system with Raman-Nath regime using 980 infrared laser and 2MHz ultrasound and the reference invasive measurements, where pn: COVID-19 patient number and n (1to4).

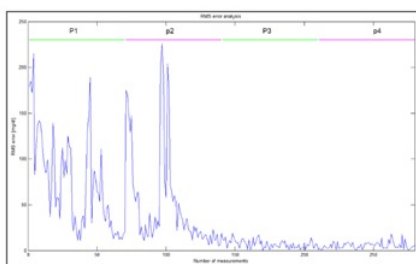


Figure 6: RMS error was calculated from the result of the experiment on four COVID-19 volunteers.

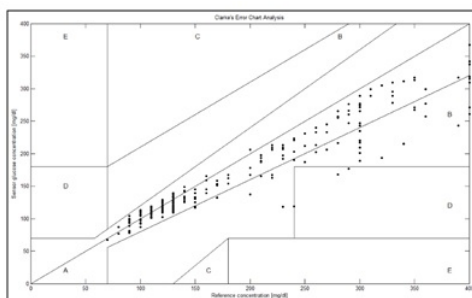


Figure 7: Clarke error chart was calculated from the result of the experiment on four COVID-19 volunteers.

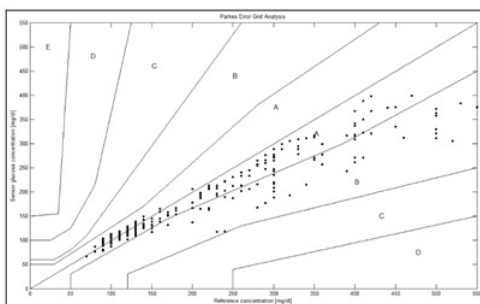


Figure 8: Parkes error grid was calculated from the result of the experiment on four COVID-19 volunteers.

## 6. Conclusion

The measurement of BGL several times a day is essential for the diagnosis and therapy of diabetes patients, especially now day diabetic COVID-19 patients, to achieve the most effective drug strategy for the diabetic patient and produce the best physiological BGL control. The noninvasive system results must be evaluated by calculating the root means square of errors and maximum errors and applying the system's measurements on Clarke and Parkes evaluation systems. Parkes error grid covers the most detecting area, and the area out of Parkes detecting is evaluated using the Parkes conditions to show drifted measurements and lead to the unprecise drug of choice. Clarke error grid shows a week evaluation due to more than 10% of the measurements being out of the Clarke detection area. The Mathematical evaluation methods (comparison or subtraction, RMS error and maximum error) fail to evaluate the new blood glucose device, unlike to Parkes evaluation system that shows promising results to this new non-invasive acousto-optic device. The AO system illustrates the simplicity of using ultrasound and near-infrared laser in the Raman-Nath regime to measure blood glucose noninvasively. The ultrasound mechanical waves enhance the glucose system sensitivity by improving the electromagnetic light penetration through the patient finger. The prototype system is applied on four COVID-19 volunteers (two of them have diabetes) and produce good evaluation results for COVID-19 patients but with a shift in the high-level measurements that may be caused by the COVID-19 effects and symptoms but also this glucose measuring prototype system (AO measuring system based on 980nm and 2MHz ultrasound) still in acceptable Parkes evaluation system. Corona pandemic accelerates the need for telemedicine technologies to monitor the glucose level of diabetic patients, especially with depression, due to staying home, which produces a dietary change and increases the intake of high-calorie food. During and after the corona pandemic, the number of diabetes patients is anticipated to rise rapidly. The interaction of people with diabetes with COVID-19 shows the importance of monitoring glucose levels several times a day or more to reach the best drug strategy for diabetic glucose management to exceed the complication related to glucose level fluctuation. Without annoying the patient with the pricking finger, especially, they suffer from depression and anxiety generated from COVID-19 complications. The non-invasive glucose detection device shows a non-contaminated diagnostic manner.

## 7. Future work

Develop a portable glucose monitoring smart device that could calculate and save glucose data and send it to another location to share the patient health information with the specialist. Developed an alarming system to alert the patient family when the glucose level passes a specific threshold to indicate hyperglycemia or hypoglycemic conditions. Developed specialist COVID-19 glucose monitoring system could measure BGL with excellent evaluation by entering correlated COVID-19 physiological parameters. Developed a numerical integrated system that could predict glucose measurements from the previously saved data and patient meals.

## References

- [1] Y. Adu-Agyeiwaah, M.B. Grant and A.G. Obukhov, *The potential role of osteopontin and furin in worsening disease outcomes in COVID-19 patients with pre-existing diabetes*, Cells 9(11) (2020) 2528.
- [2] C. Akarsu, M. Karabulut, H. Aydin, N.A. Sahbaz, A.C. Dural, D. Yegul and G.T. Adas, *Association between acute pancreatitis and COVID-19: could pancreatitis be the missing piece of the puzzle about increased mortality rates?*, J. Invest. Surgery 35 (2020) 1–7.
- [3] L.N. Bachache, J.A. Hasan and A.Q. Al-Neami, *Acousto-optic Design to Measure Glucose Level for Diabetic Patients Non-invasively*, In J. Phys. Conf. Ser. 1818(1) (2021) 012147.

- [4] Z.T. Bloomgarden, *Diabetes and COVID-19*, J. Diabetes 12(4) (2020) 347–348.
- [5] M.M. Burlaw, E.L. Madsen, J.A. Zagzebski, R.A. Banjavic and S.W. Sum, *A new ultrasound tissue-equivalent material*, Radiol. Phys. J. 134(2) (1980) 517–520.
- [6] E.N. Carlsen, *Ultrasound physics for the physician a brief review*, J. Clinic. Ultrasound 3 (1975) 69–75.
- [7] Y. Cheng, L. Yue, Z. Wang, J. Zhang and G. Xiang, *Hyperglycemia associated with lymphopenia and disease severity of COVID-19 in type 2 diabetes mellitus*, J. Diabetes . Compl. 35(2) (2021) 107809.
- [8] W.L. Clarke, *The original Clarke error grid analysis (EGA)*, Diabetes Technol. Therap. 7(5) (2005) 776–779.
- [9] D.J. Cox, L.A. Gonder-Frederick, B.P. Kovatchev, D.M. Julian and W.L. Clarke, *Understanding error grid analysis*, Diabetes Care 20(6) )1997( 911.
- [10] G. Jin, X. Zhang, W. Fan, Y. Liu and P. He, *Design of non-contact infrared thermometer based on the sensor of MLX*, Open Autom. Control Syst. J. 7(1) (2015) 8–20.
- [11] S. Gläser, S. Krüger, M. Merkel, P. Bramlage and F.J. Herth, *Chronic obstructive pulmonary disease and diabetes mellitus: a systematic review of the literature*, Respiration 89(3) (2015) 253–264.
- [12] I. Kapoor, H. Prabhakar and C. Mahajan, *Introduction: History of Coronavirus Disease Pandemic*, Clinical Synopsis of COVID-19, Springer, Singapore, (2020) 1–4.
- [13] S.A. Lee, M.C. Jobe, A.A. Mathis, J.A. Gibbons, *Incremental validity of coronaphobia: Coronavirus anxiety explains depression*, J. Anxiety Disord 74 (2020) 102268.
- [14] J.A. McGrath, R.A.J. Eady and F.M. Pope, *Anatomy and organization of human skin*, Rook's Textbook of Dermatology 1 (2016) 2–3.
- [15] Melexis inspired engineering, *Datasheet Single and Dual Zone Infra Red Thermometer in TO-39*, MLX90614 family datasheet, 2019.
- [16] E. Merzon, I. Green, M. Shpigelman, S. Vinker, I. Raz, A. Golan-Cohen and R. Eldor, *Haemoglobin A1c is a predictor of COVID-19 severity in patients with diabetes*, Diabetes/metabol. Res. Rev. 37(5) (2021) e3398.
- [17] S. Nazar Haddad and R. Istepanian, *A feasibility study of mobile phone text messaging to support education and management of type 2 diabetes in Iraq*, Diabetes Technol. Therap. 16(7) (2014) 454–459.
- [18] F.J. Pasquel and G.E. Umpierrez, *Individualizing inpatient diabetes management during the Coronavirus disease 2019 pandemic*, J. Diabetes Sci. Technol. 14(4) (2020) 705–707.
- [19] M.C. Petersen G.I. Shulman, *Mechanisms of insulin action and insulin resistance*, Physiol. Rev. 98(4) (2018) 2133–2223.
- [20] A. Pfützner, D.C. Klonoff, S. Pardo and J.L. Parkes, *Technical aspects of the Parkes error grid*, J. Diabetes Sci. Technol. 7(5) (2013) 1275–1281.
- [21] B. Shirin, *Diabetes mellitus and gestational diabetes mellitus*, J. Paediatric Surg. Bangl. 5(1) (2015) 30–35.
- [22] A.K. Singh, R. Gupta, A. Ghosh and A. Misra, *Diabetes in COVID-19: Prevalence, pathophysiology, prognosis and practical considerations*, Diabetes Metab Syndr. 14(4) (2020) 303–310.
- [23] A.K. Singh, R. Gupta, A. Ghosh and A. Misra, *Diabetes in COVID-19: Prevalence, pathophysiology, prognosis and practical considerations*, Diabetes Metabol. Syndr. Clinical Res. Rev. 14(4) (2020) 303–310.
- [24] G. Wilcox, *Insulin and insulin resistance*, Clinical Bioch. Rev. 26(2) (2005) 19.